General-relativistic pulsar magnetospheres

Jérôme Pétri[1]

[1]Observatoire astronomique de Strasbourg, Université de Strasbourg, France.

Summary

Our goal

1. **Objectives**
   to construct pulsar magnetospheres
   - in general-relativity.
   - force-free limit.
   - extension to dissipative/resistive/MHD solutions.
2. **Method**
   full 3D numerical simulations
   - time-dependent evolution of the electromagnetic field.
   - 3+1 formalism in general relativity.
   - spherical coordinate system.
   - pseudo-spectral discontinuous Galerkin approximation.
3. **Applications**
   plasma physics in curved space-time
   - pulsar.
   - magnetar.
   - black holes.

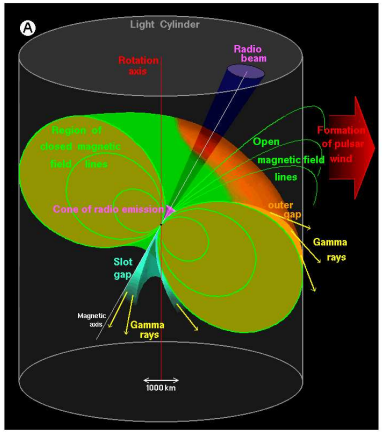

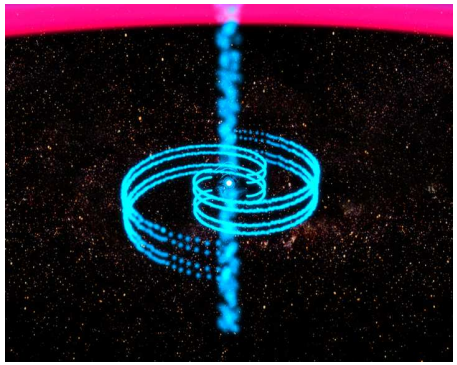

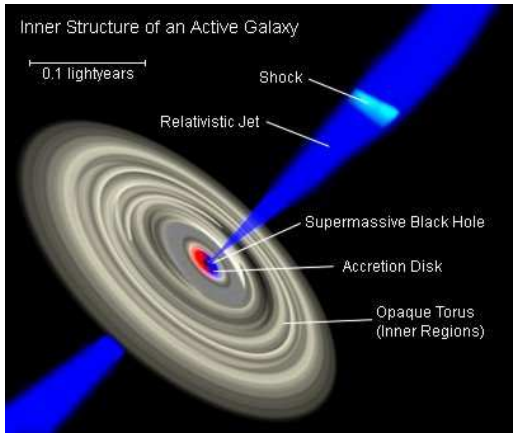

Force-free magnetospheres

- Almost FFE simulation
  - force-free electromagnetic field.
  - time evolution of Maxwell equations.
  - current along **B** not included.
  - formation of a current sheet.
- Limitations
  - cartesian geometry even for the star surface.
  - ratio $R/r_{\mathrm{L}} = 0.2$ too large $\Rightarrow$ $P = 1$ ms.
  - strong gravitational field effects not extensively investigated.
- Remedies

  $\Rightarrow$ use spherical geometry and pseudo-spectral methods

  2D axisymmetric (Parfrey et al., 2012)

  full 3D geometry (Pétri, 2012)

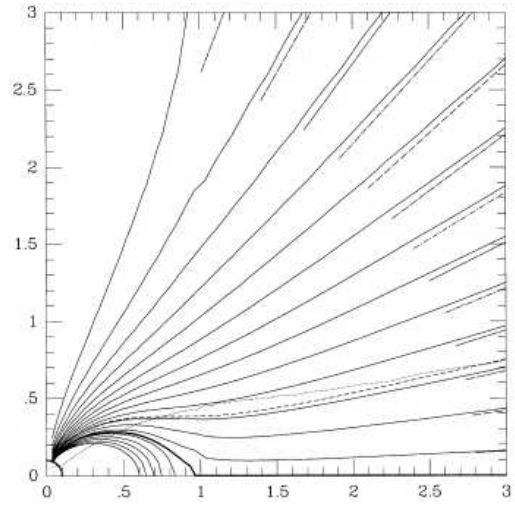

(Contopoulos et al., 1999)

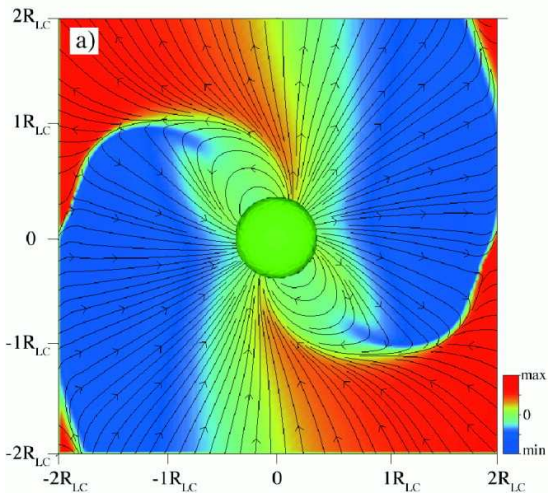

(Spitkovsky, 2006)

General-relativistic effects

Space-time curvature and frame dragging

modify the structure of the electromagnetic field close to the neutron star surface

- amplification of the intensity of the electric field in the neighborhood of the stellar surface because of the gravitational field
  (Muslimov & Tsygan, 1992).
- dynamics of the polar caps changed
  (Beskin, 1990).

Consequences on the magnetosphere

Quantitative modifications of

- the geometry of the polar caps, opening angle.
- the shape of the radio pulses.
- the modulation of the light-curves in X-rays for accreting pulsars.
- spin-down luminosity.
  (Pétri, 2013, 2014).

The background metric

Four dimensional space-time splitted into a 3+1 foliation such that

$$ds^2 = g_{ik}\, dx^i\, dx^k = \alpha^2\, c^2\, dt^2 - \gamma_{ab}\, (dx^a + \beta^a\, c\, dt)\, (dx^b + \beta^b\, c\, dt)$$

with coordinate basis $x^i = (c\, t, x^a)$, t is the time coordinate or universal time and x^a some associated space coordinates.

- lapse function α.
  For a slowly rotating neutron star

$$\alpha = \sqrt{1 - \frac{R_s}{r}}$$

  Schwarzschild radius $R_s = 2\, G\, M / c^2$.

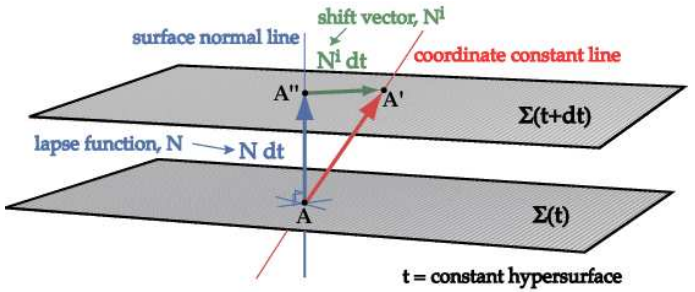

(Shinkai, 2009)

- shift vector β

$$c\, \beta = -\, \omega\, r\, \sin\vartheta\, \vec{e}_\varphi$$

$$\omega = \frac{R_s\, a\, c}{r^3}$$

Maxwell equations in 3+1 formalism

Maxwell equations in curved space-time are similar to those in matter

$$\begin{aligned}
\mathrm{div}\,\mathbf{B} &= 0 \\
\mathbf{rot}\,\mathbf{E} &= -\frac{1}{\sqrt{\gamma}}\,\partial_t(\sqrt{\gamma}\,\mathbf{B}) \\
\mathrm{div}\,\mathbf{D} &= \rho \\
\mathbf{rot}\,\mathbf{H} &= \mathbf{J} + \frac{1}{\sqrt{\gamma}}\,\partial_t(\sqrt{\gamma}\,\mathbf{D})
\end{aligned}$$

(Komissarov, 2004)

Differential operators defined in a three dimensional curved space, the absolute space with associated spatial metric γ_{ab}

$$\begin{aligned}
\mathrm{div}\,\mathbf{B} &\equiv \frac{1}{\sqrt{\gamma}}\,\partial_a(\sqrt{\gamma}\,B^a) \\
\mathbf{rot}\,\mathbf{E} &\equiv e^{abc}\,\partial_b\,E_c \\
\mathbf{E}\times\mathbf{B} &\equiv e^{abc}\,E_b\,B_c
\end{aligned}$$

Constitutive relations

- three dimensional vector fields are not independent, they are related by two important constitutive relations

$$\varepsilon_0 \, \mathbf{E} = \alpha \, \mathbf{D} + \varepsilon_0 \, c \, \beta \times \mathbf{B}$$

$$\mu_0 \, \mathbf{H} = \alpha \, \mathbf{B} - \frac{\beta \times \mathbf{D}}{\varepsilon_0 \, c}$$

- curvature of absolute space taken into account by
  - lapse function factor α in the first term.
  - frame dragging effect in the second term, cross-product between the shift vector β and the fields.
- $(\mathbf{D}, \mathbf{B})$ are the fundamental fields measured by a FIDO. The force-free current density is

$$\mathbf{J} = \rho \, \frac{\mathbf{E} \times \mathbf{B}}{B^2} + \frac{\mathbf{B} \cdot \mathbf{rot} \, \mathbf{H} - \mathbf{D} \cdot \mathbf{rot} \, \mathbf{E}}{B^2} \, \mathbf{B}$$

$$\alpha \, \mathbf{j} = \mathbf{J} + \rho \, c \, \beta$$

Numerical method

Pseudo-spectral discontinuous Galerkin method

- finite volume formulation in radius.
- high-order interpolation with Legendre polynomials.
- non uniform radial grid (high resolution where needed).
- spectral interpolation in longitude/latitude.
- vector spherical harmonic decomposition.
- 4th order Runge-Kutta time integration.
- Lax-Friedrich flux.
- stabilization by filtering and limiting (avoid overshoot/oscillations).
- exact boundary conditions on the neutron star surface.
- outgoing waves at the outer boundary.

Tested against

- vacuum monopole and Deutsch solution.
- force-free monopole/split monopole.

(Pétri, 2012)

Vacuum perpendicular solutions

Poynting flux for the perpendicular rotator in flat space-time

$$L_{\rm dip} = \frac{8\,\pi}{3\,\mu_0\,c^3}\,\Omega^4\,B^2\,R^6 \qquad (5)$$

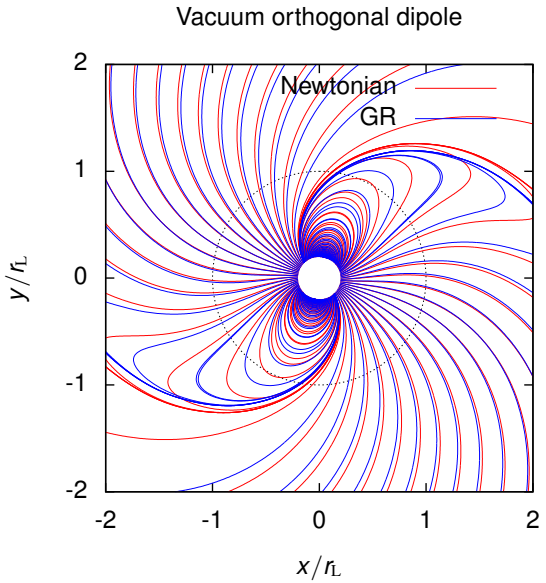

Figure : Magnetic field lines in the equatorial plane for $r_{\rm L}/R = 10$.

(Pétri, 2016)

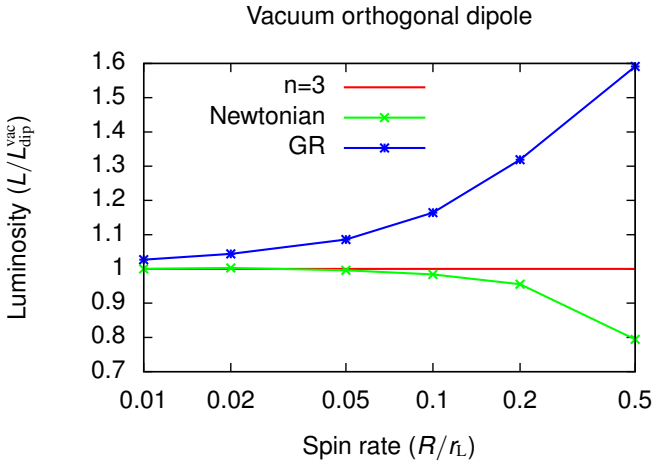

Figure : Poynting flux $L/L_{\rm dip}$ compared to the Deutsch solution. (Corrections for Ω-redshift and B-amplification omitted, see (Rezzolla & J. Ahmedov, 2004)).

Spin parameter

$$\frac{a}{R_{\rm s}} = \frac{2}{5}\,\frac{R}{R_{\rm s}}\,\frac{R}{r_{\rm L}}$$

with $R = 2\,R_{\rm s}$.

Vacuum oblique solutions

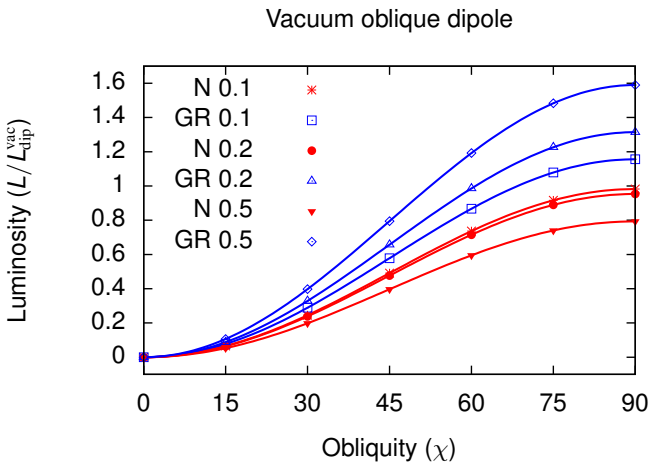

Figure : Poynting flux of the vacuum oblique rotator for different obliquities χ and normalized to $L_{\rm dip}^{\rm vac}$ with $R/r_{\rm L} = \{0.1, 0.2, 0.5\}$.

(Pétri, 2016)

$R/r_{\rm L}$	Newtonian	GR
0.1	0.982	1.156
0.2	0.955	1.316
0.5	0.793	1.590

Table : Best fit parameter b for the Poynting flux $L(\chi)/L_{\rm dip}^{\rm vac} = b \sin^2\chi$ of the vacuum dipole rotator in Newtonian and general-relativistic case.

Spin parameter

$$\frac{a}{R_{\rm s}} = \frac{2}{5}\,\frac{R}{R_{\rm s}}\,\frac{R}{r_{\rm L}}$$

with $R = 2\,R_{\rm s}$.

Aligned dipole: magnetic field and Poynting flux

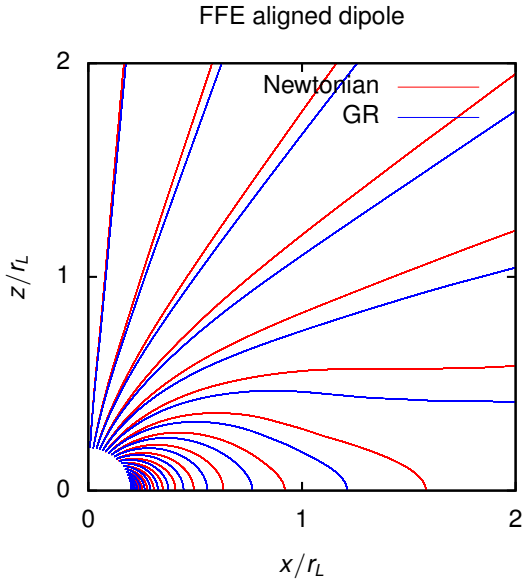

Figure : Meridional field lines in flat space-time, red solid line, and in GR, blue solid line, with $R/r_{\rm L} = 0.2$.

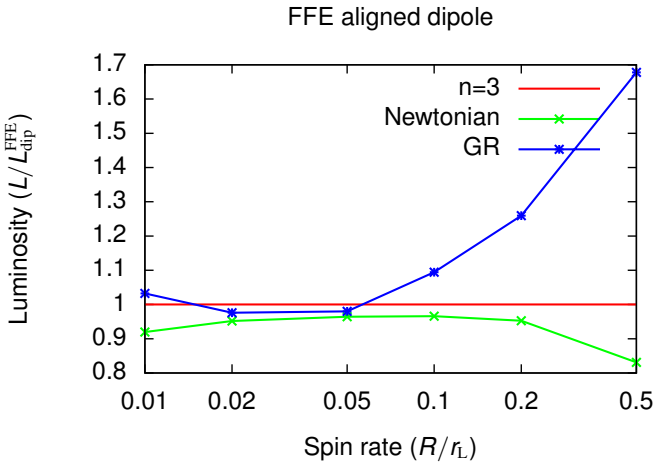

Figure : Poynting flux of the force-free aligned rotator for $R/r_{\rm L} = \{0.01, 0.02, 0.05, 0.1, 0.2, 0.5\}$ and normalized to $L_{\rm dip}^{\rm FFE}$.

$$L_{\rm dip}^{\rm FFE} = \frac{3}{2} L_{\rm dip}^{\rm vac}$$

(Pétri, 2016)

Perpendicular dipole: magnetic field and Poynting flux

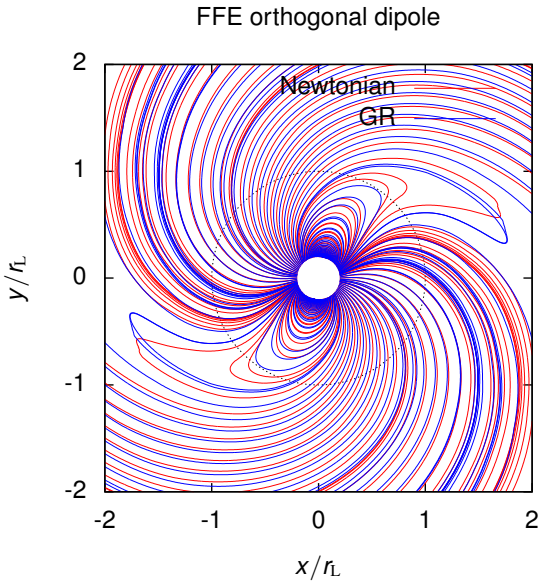

Figure : Force-free magnetic field lines of the perpendicular rotator in the equatorial plane for $r_{\rm L}/R = 10$.

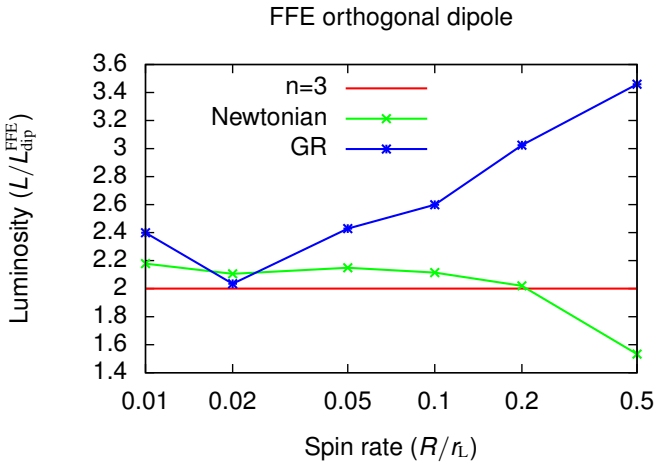

Figure : Poynting flux of the force-free orthogonal rotator normalized to $L_{\rm dip}^{\rm FFE}$ and for $R/r_{\rm L} = \{0.01, 0.02, 0.05, 0.1, 0.2, 0.5\}$.

(Pétri, 2016)

FFE oblique solutions

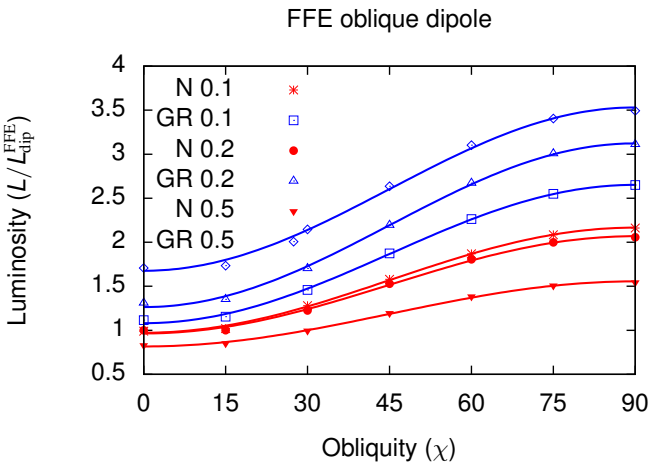

Figure : Poynting flux of the force-free oblique rotator for different obliquities χ and normalized to $L_{\rm dip}^{\rm FFE}$.

(Pétri, 2016)

$R/r_{\rm L}$	Newtonian	GR
0.1	0.972 / 1.193	1.080 / 1.570
0.2	0.847 / 1.184	0.946 / 2.094
0.5	0.818 / 0.737	1.650 / 1.888

Table : Best fit parameters a/b for the Poynting flux of the FFE dipole rotator in Newtonian and GR cases.

Spin parameter

$$\frac{L(\chi)}{L_{\rm dip}^{\rm FFE}} = a + b\,\sin^2\chi$$

Conclusions & Perspectives

Vacuum and force-free fields

- fully 3D general-relativistic force-free pulsar magnetosphere.
- spin-down luminosity increased by a significant amount compared to flat space-time.
- be careful about the point dipole magneto-losses formula.
- phase lag in the magnetic field structure
  $\Rightarrow$ implications for radio and high-energy pulse phase lag?
- braking index is always $n \approx 3$.

Magnetospheres of compact objects

- more realistic assumptions for the plasma
  $\Rightarrow$ relaxation of the force-free condition: dissipation, radiation reaction.
- GRMHD simulations.
- resistive magnetospheres.

Bibliography

Beskin V. S., 1990, Soviet Astronomy Letters, 16, 286

Contopoulos I., Kazanas D., Fendt C., 1999, ApJ, 511, 351

Komissarov S. S., 2004, MNRAS, 350, 427

Muslimov A. G., Tsygan A. I., 1992, MNRAS, 255, 61

Parfrey K., Beloborodov A. M., Hui L., 2012, MNRAS, 423, 1416

Pétri J., 2012, MNRAS, 424, 605

Pétri J., 2013, MNRAS, 433, 986

Pétri J., 2014, MNRAS, 439, 1071

Pétri J., 2016, MNRAS, 455, 3779

Rezzolla L., J. Ahmedov B., 2004, MNRAS, 352, 1161

Shinkai H., 2009, Journal of Korean Physical Society, 54, 2513

Spitkovsky A., 2006, ApJL, 648, L51